Electronic Supplementary Material (ESI) for Journal of Materials Chemistry C.
This journal is © The Royal Society of Chemistry 2024

Supporting Information

Reversible nonvolatile control of anomalous valley Hall effect in two-dimensional multiferroic materials based on $GdGe_2$

Xuhong Li[1], Jiawei Li[2], Zhihao Gao[1], Ziyu Niu[1], Xinyue Bi[1], Jinwei Gao[1], Tengfei Cao[1] and Xiaoli Fan[1]*

[1] *State Key Laboratory of Solidification Processing, Center for Advanced Lubrication and Seal Materials, School of Material Science and Engineering, Northwestern Polytechnical University, 127 YouYi Western Road, Xi'an, Shaanxi 710072, China.*

[2] *Queen Mary University of London Engineering School, Northwestern Polytechnical University, 127 YouYi Western Road, Xi'an, Shaanxi 710072, China*

*Corresponding author: xlfan@nwpu.edu.cn

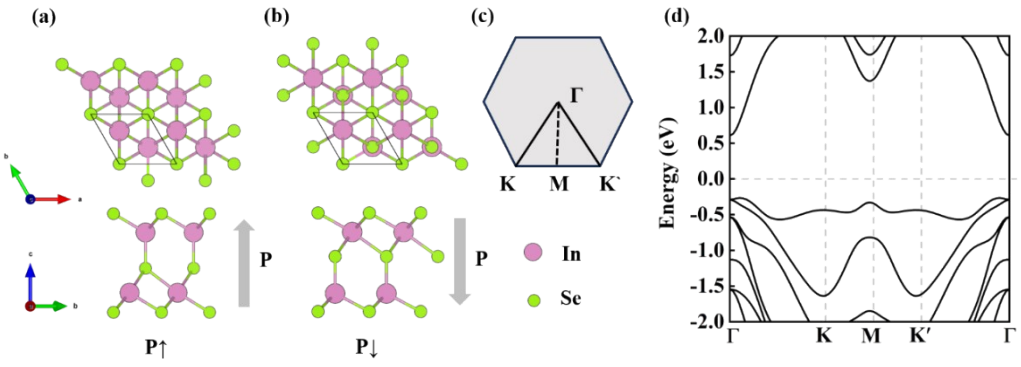

Figure S1. Top and side views for the atomic structures of monolayer In_2Se_3 with the electric polarization along (a) upward (In_2Se_3↑) and (b) downward (In_2Se_3↓) direction. The black rhombi marks the unit cell. (c) First Brillouin zone of monolayer $GdGe_2$ and In_2Se_3 marking with the high symmetric points. (d) Electronic band structure of monolayer In_2Se_3.

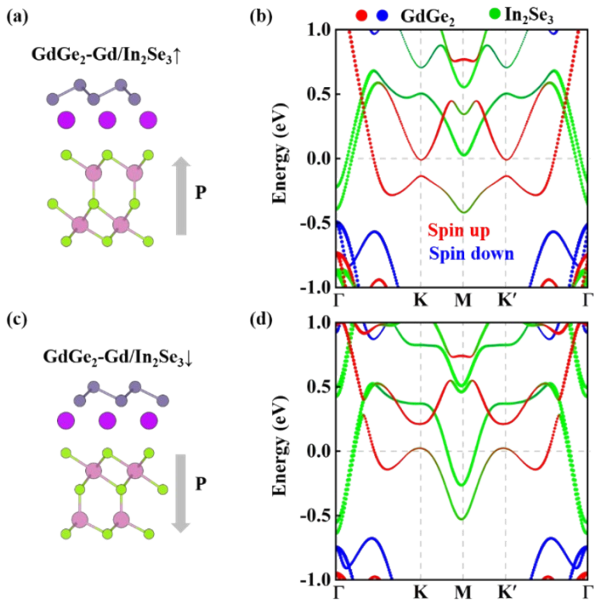

Figure S2. Side views for the atomic structures of $GdGe_2/In_2Se_3$ heterojunction with the Gd atomic layer of $GdGe_2$ at the interface and electric polarization of In_2Se_3 along the direction pointing (a) toward ($GdGe_2$-Gd/In_2Se_3↑) and (c) backward ($GdGe_2$-Gd/In_2Se_3↓) the $GdGe_2$ monolayer. Electronic band structures of (b) $GdGe_2$-Gd/In_2Se_3↑ and (d) $GdGe_2$-Gd/In_2Se_3↓ heterojunctions without considering the spin orbit coupling (SOC).

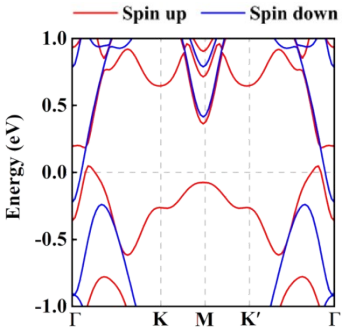

Figure S3. Electronic band structure of $GdGe_2$-Ge/In_2Se_3↓ heterojunction calculated using the HSE method.

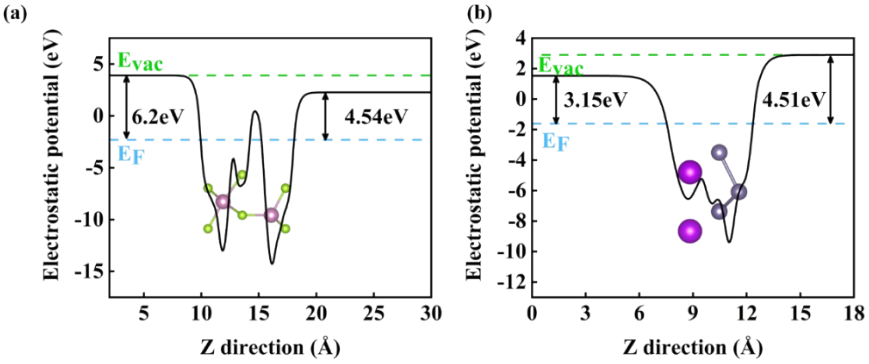

Figure S4. The evolution of the xy-plane-averaged electrostatic potential along z direction for monolayer (a) In_2Se_3 and (b) $GdGe_2$. E_{vac} represents the vacuum energy level, and E_F represents the Fermi energy level.

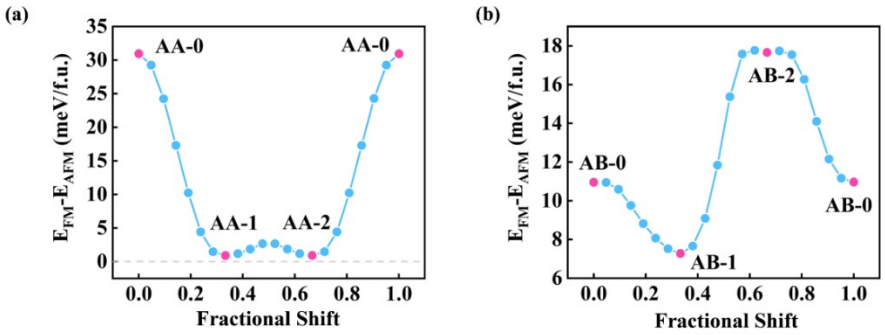

Figure S5. Evolution of the interlayer magnetic exchange energy of bilayer $GdGe_2$ with respect to the in-plane translation of the top $GdGe_2$ monolayer along the $[1\bar{1}0]$ direction starting from (a) the AA-0 and (b) the AB-0 stacking.

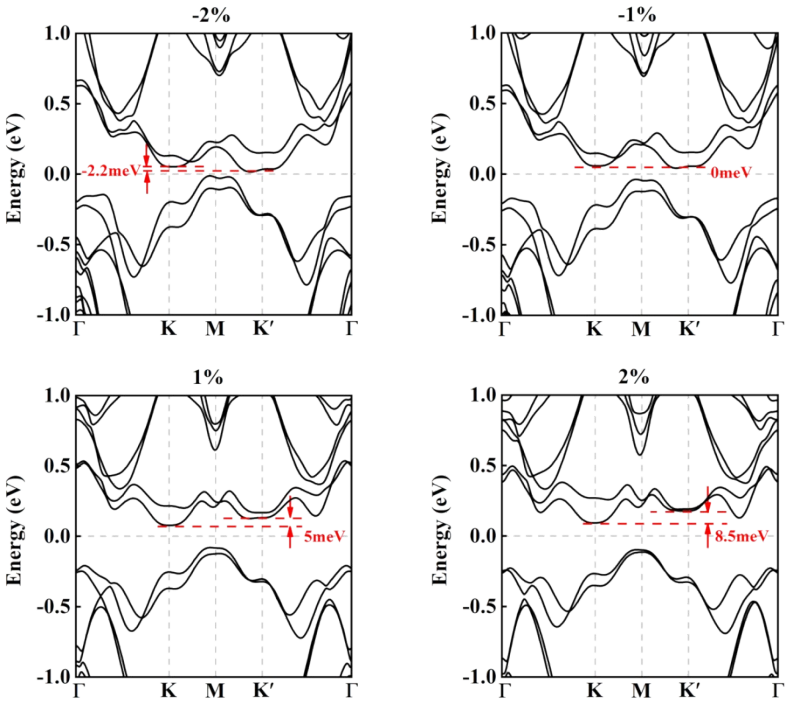

Figure S6. Electronic band structures of AA-2 stacking under the biaxial strain of -2 ~ 2% with considering the spin orbital coupling (SOC).

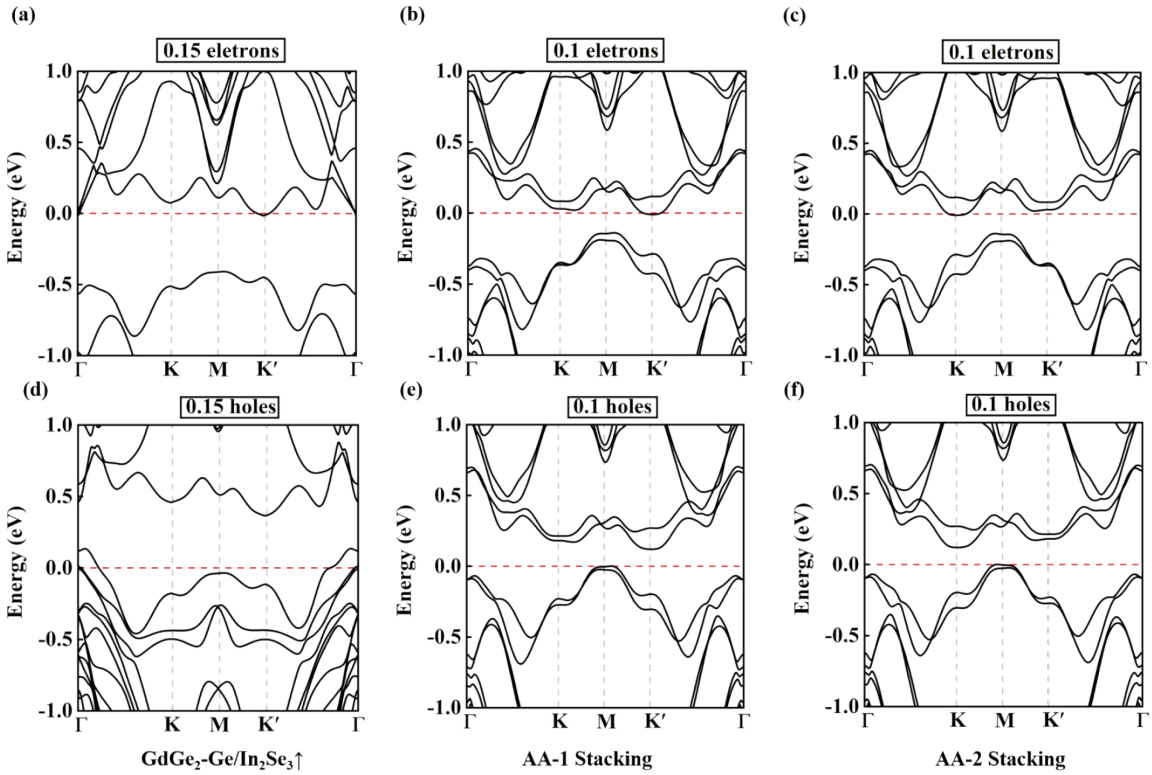

Figure S7. Electronic band structures of (a) $GdGe_2$-Ge/In_2Se_3↑ with 0.15 electrons doping, (b) AA-1 stacking bilayer $GdGe_2$ with 0.1 electrons doping, (c) AA-2 stacking bilayer $GdGe_2$ with 0.1 electrons doping. Electronic band structures of (d) $GdGe_2$-Ge/In_2Se_3↑, (e) AA-1 stacking bilayer $GdGe_2$, and (f) AA-2 stacking bilayer $GdGe_2$ with 0.1 holes doping.

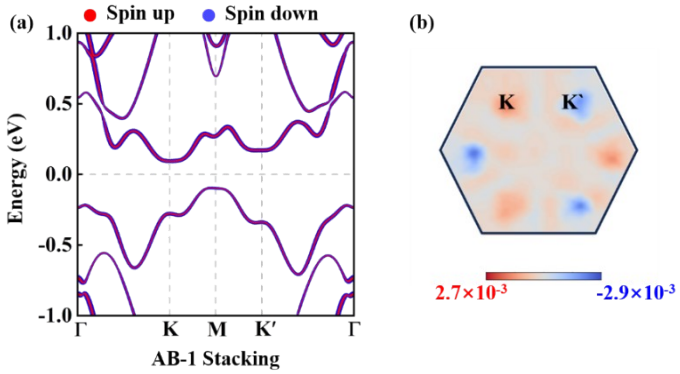

Figure S8. (a) Electronic band structures of AB-1 stacking bilayer $GdGe_2$ with considering the spin orbital coupling (SOC). (c) Berry curvatures of AB-1 stacking bilayer $GdGe_2$ in the whole 2D Brillouin zone.